Electron-impact ionization of the boron atom

J. C. Berengut, S. D. Loch, and M. S. Pindzola
Department of Physics, Auburn University, Auburn, Alabama 36849, USA

C. P. Ballance and D. C. Griffin
Department of Physics, Rollins College, Winter Park, Florida 32789, USA

(Received 29 May 2007; published 5 October 2007)

Accurate knowledge of the electron-impact ionization of the B atom is urgently needed in current fusion plasma experiments to help design ITER wall components. Since no atomic measurements exist, nonperturbative time-dependent close-coupling (TDCC) calculations are carried out to accurately determine the direct ionization cross sections of the outer two subshells of B. Perturbative distorted-wave and semiempirical binary encounter calculations are found to yield cross sections from 26% lower to an order of magnitude higher than the current TDCC results. Unlike almost all neutral atoms, large excitation-autoionization contributions are found for the B atom. Nonperturbative *R* matrix with pseudostates (RMPS) calculations are also carried out to accurately determine the total ionization cross section of B. Previous 60 LS-term RMPS calculations are found to yield cross sections up to 40% higher than the current more extensive 476 LS-term RMPS results.

DOI: 10.1103/PhysRevA.76.042704 PACS number(s): 34.80.Dp, 52.20.Hv

Determination of the proper selection of plasma facing components for ITER and subsequent power-producing fusion reactors remains a challenging research area [1]. Low Z materials, such as Li, Be, B, and C, have the advantage that they rapidly ionize and cannot contribute to radiative power loss in the central plasma core. On the other hand, high Z materials such as Mo and W, have advantages with respect to withstanding neutron damage and erosion, as well as having lower levels of tritium retention. In particular, enhanced energy confinement in current tokamak experiments has been achieved by coating heavy metal facing components with boron [2,3]. A key atomic process in understanding plasma performance is the electron ionization of B leading to spectral emission of B ions at the plasma edge.

In recent years, nonperturbative converged close coupling, time-dependent close coupling, and R matrix with pseudostates methods have been used to calculate accurate electron-impact direct ionization cross sections for both neutral Li [4] and Be [5,6]. A perturbative distorted-wave method was found to yield peak cross sections 50% higher than the more accurate nonperturbative methods for ionization from the Li($1s^2 2s$) ground configuration. Perturbative distorted-wave methods were also found to yield peak cross sections from 35% to 55% higher than the more accurate nonperturbative methods for ionization from the Be($1s^2 2s^2$) ground configuration. For both Li and Be all three nonperturbative methods are in excellent agreement with respect to their predictions of ionization cross sections dominated by the direct "knock-out" process.

In this paper, we use the nonperturbative time-dependent close-coupling (TDCC) and R-matrix with pseudostates (RMPS) methods to calculate accurate electron-impact ionization cross sections for neutral B, for which no atomic measurements exist. Although accurate atomic collision calculations are much more difficult for the B($1s^2 2s^2 2p$) ground configuration due to the presence of three active electrons above the $1s^2$ core, implementation of the TDCC and RMPS methods on current large scale computing platforms has now allowed studies of this more complex scattering system. The TDCC method is used to determine the direct ionization cross sections of the outer two subshells of the B($1s^2 2s^2 2p$) ground configuration. Comparison is made with various perturbative distorted-wave and semiempirical binary encounter [7] calculations of the direct ionization of the $2p$ and $2s$ subshells. The comparison is found to highlight the absence of shape resonances predicted by a distorted-wave method employing a mixture of V^N and V^{N-1} scattering potentials, and to also highlight the importance of the quantal three-body Coulomb interaction effects included in the nonperturbative TDCC method. Unlike almost all neutral atoms, large excitation-autoionization contributions are found for the B atom. Various plane-wave Born [7], single configuration distorted-wave, and multiconfiguration distorted-wave [8] calculations are compared for the strong dipole allowed $1s^2 2s^2 2p\ ^2P^o \rightarrow 1s^2 2s 2p^2\ ^2P^e$ transition that lies only 0.7 eV above the $2p$ ionization threshold. The comparison highlights the difficulty in predicting accurate excitation cross sections to excited states near the ionization threshold in neutral atoms. Finally, a 476 LS-term RMPS method is used to determine the total ionization cross section for the B($1s^2 2s^2 2p$) ground configuration. An RMPS calculation used recently to calculate various excitation cross sections [9] is modified here to calculate the total ionization cross section for B. Comparison is made with the TDCC direct ionization cross section results and previous 60 LS-term RMPS total ionization cross section results [10] to highlight the true size of the excitation autoionization contributions and the effect of including a large number of LS terms in a $1s^2 2s^2 nl$, $1s^2 2s 2pnl$, and $1s^2 2p^2 nl$ close-coupling expansion. In the paragraphs below, unless otherwise stated, all quantities are given in atomic units.

To obtain the TDCC results, the time-dependent Schrödinger equation is converted into a set of close-coupled partial differential equations (see, e.g., Ref. [11]). These are solved for each LS symmetry on a two dimensional radial lattice. The Hamiltonian contains the kinetic energy, nuclear

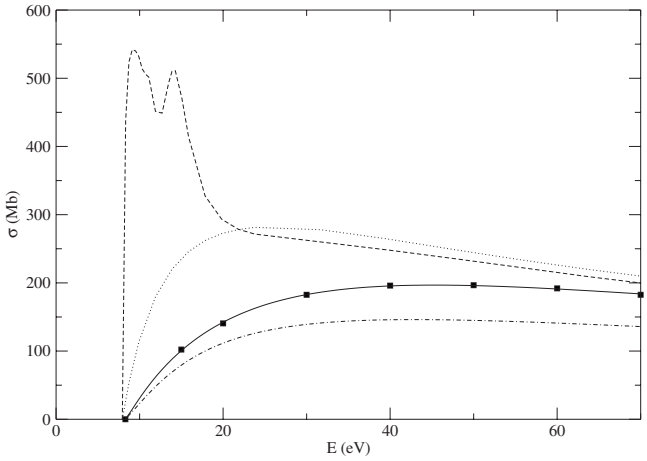

FIG. 1. Electron-impact direct ionization cross section for the $2p$ subshell of the B($1s^2 2s^2 2p$) ground configuration. Filled squares connected by solid line: TDCC method, dashed line: mixed V^N/V^{N-1} potential distorted-wave method, dotted line: strictly V^{N-1} potential distorted-wave method, dot-dashed line: semiempirical binary encounter method [7]. (1 Mb=10^{-18} cm^2.)

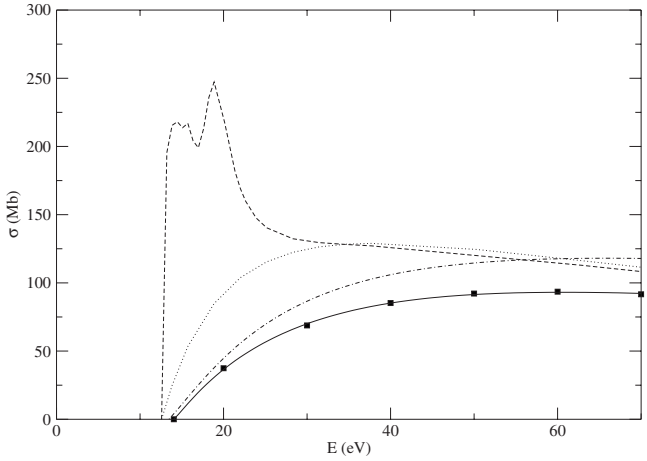

FIG. 2. Electron-impact direct ionization cross section for the $2s$ subshell of the B($1s^2 2s^2 2p$) ground configuration. Filled squares connected by solid line: TDCC method, dashed line: mixed V^N/V^{N-1} potential distorted-wave method, dotted line: strictly V^{N-1} potential distorted-wave method, dot-dashed line: semiempirical binary encounter method [7]. (1 Mb=10^{-18} cm^2.)

potential, and core Hartree-exchange potential operators, as well as the full Coulomb repulsion operator between the two active electrons. The initial condition for the TDCC solution is given by a product of the active bound orbital and a Gaussian radial wave packet well separated spatially from the core. The cross section is obtained by extracting the partial collision probabilities from the fully time-evolved wave functions using momentum space projection methods. The TDCC calculations were carried out for all the ^1L and ^3L symmetries for both even and odd parity from $L=0$ to $L=6$, with the number of coupled channels ranging from 4 for $L=0$ to 18 for $L=6$. We employed two-dimensional lattices ranging from 192 to 384 points in each dimension and uniform mesh spacings ranging from $\Delta r=0.10$ to $\Delta r=0.20$. Since good agreement was found between the TDCC and distorted-wave partial cross sections for $L=6$, distorted-wave calculations for $L=7$ to $L=25$ were used to "top-up" the low L TDCC results.

Total integral cross sections for the electron-impact direct ionization of the $2p$ and $2s$ subshells of the B($1s^2 2s^2 2p$) ground configuration are presented in Figs. 1 and 2. We note that direct single ionization cross sections, whether calculated perturbatively or nonperturbatively, are only weakly dependent on initial state correlation effects [6]. The TDCC calculations were carried out at incident energies between 15 and 70 eV, as shown by the solid squares in the figures. The mixed V^N/V^{N-1} potential distorted-wave calculations [12,13] exhibit large V^N potential shape resonances in complete disagreement with the nonperturbative TDCC results for both subshells. The shape resonances observed for the B atom are due to the direct part of the core electrostatic potential and its effect on the p, d, and f electron continuum radial orbitals, as opposed to those due to term-dependent exchange potentials seen in the electron ionization of closed subshells [14].

The distorted-wave calculations were repeated using the strictly V^{N-1} potential method [15], which eliminates the low partial wave V^N shape resonances. Although the agreement between the distorted-wave and TDCC results has greatly improved, at 20 eV incident energy the strictly V^{N-1} potential distorted-wave results are still a factor of 1.9 higher than the TDCC results for the $2p$ subshell and a factor of 2.3 higher than the TDCC results for the $2s$ subshell. The mixed V^N/V^{N-1} potential and strictly V^{N-1} potential versions of the distorted-wave method are generally in good agreement for the electron ionization of multiply charged atomic ions. In the case of the electron ionization of the neutral Fe atom, experiment clearly ruled in favor of no V^N shape resonances [16], while here again in the case of the electron ionization of the neutral B atom, the nonperturbative TDCC method rules in favor of no V^N shape resonances. The semiempirical binary encounter calculations [7] yield direct ionization cross sections that are in better agreement with the nonperturbative TDCC results than the strictly V^{N-1} potential distorted-wave results. At 50 eV incident energy, the semiempirical binary encounter results are 26% lower than the TDCC results for the $2p$ subshell and 25% higher than the TDCC results for the $2s$ subshell. Finally, we note that the total direct ionization cross section for B (summing the $2s$ and $2p$ subshell contributions) predicted by the semiempirical binary encounter method [7] and from scaling ionization data along the isoelectronic sequence [17] are both in reasonable agreement with the TDCC results.

Unlike almost all neutral atoms, large excitation-autoionization contributions are found for electron ionization of the B atom. Excitation cross sections for the $1s^2 2s^2 2p\ ^2P^o \rightarrow 1s^2 2s 2p^2\ ^2P^e$ transition are shown in Fig. 3. This strong dipole transition lies only 0.7 eV above the $2p$ ionization threshold. For all other atomic ions in the B isonuclear sequence, the $^2P^e$ term is bound. We compare our unitarized LS-resolved calculation with bound Hartree-Fock orbitals from the single $1s^2 2s^2 2p$ configuration with previous plane-wave Born [7] and multiconfiguration distorted-wave

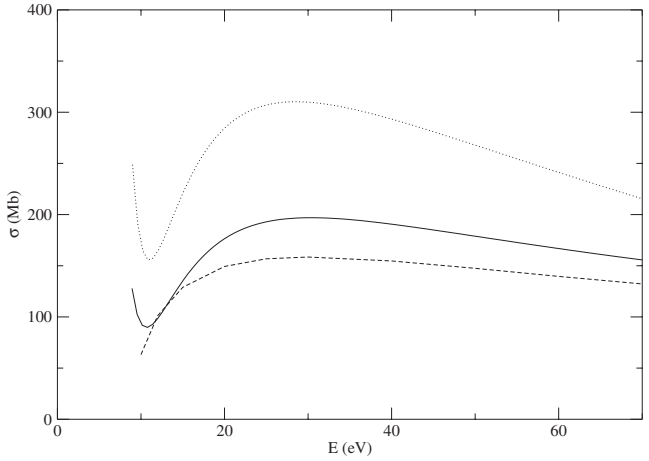

FIG. 3. Electron-impact excitation cross section for the $1s^22s^22p\ ^2P^o \rightarrow 1s^22s2p^2\ ^2P^e$ transition in B. Solid line: multiconfiguration distorted-wave method [8], dotted line: single configuration unitarized distorted-wave method, dashed line: plane-wave Born method [7]. (1 Mb=10^{-18} cm^2.)

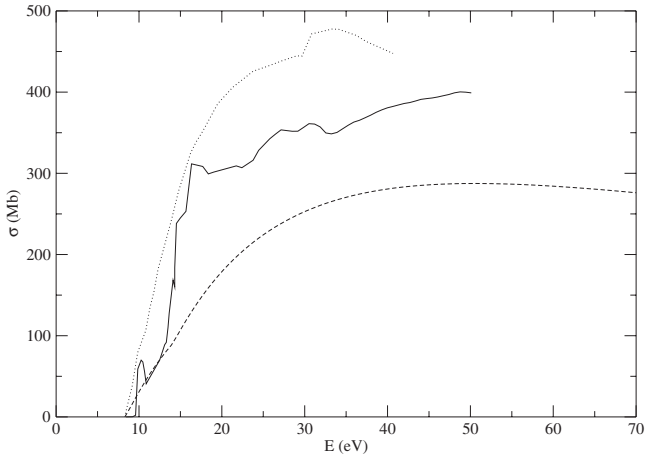

FIG. 4. Electron-impact total ionization cross section for the $B(1s^22s^22p)$ ground configuration. Solid line: 476 LS-term RMPS method, dashed line: TDCC method for direct ionization of the $2p$ and $2s$ subshells, dotted line: 60 LS-term RMPS method [10]. (1 Mb=10^{-18} cm^2.)

[8] calculations. The substantial difference between our single-configuration distorted-wave results and the previous multiconfiguration distorted-wave results [8] is most likely due to target configuration-interaction effects, as we found in the RMPS calculations reported in the following paragraphs for the total ionization cross section. Of course, all the cross section calculations shown in Fig. 3 ignore the strong coupling between the excited states that lie both below and above the $2p$ ionization threshold as well as coupling of the autoionizing states with the adjacent continuum. We also note that further excitation cross sections involving the $1s^22s^22p \rightarrow 1s^22s2pnl$ transitions for $n \geqslant 3$ must be included in a complete calculation for the indirect ionization contribution in B.

Nonperturbative calculations for the total ionization cross section of the B atom are carried out using the RMPS method. The target radial wave functions were calculated using the atomic structure code called AUTOSTRUCTURE [18]. The $1s$ to $4f$ spectroscopic orbitals were determined using a Thomas-Fermi-Dirac-Amaldi approximation. The $5s$ to $11g$ Laguerre pseudo-orbitals were orthogonalized to the spectroscopic orbitals and to each other. To provide a good representation of the N-electron target and a sufficient density of pseudostates from the ionization threshold to 50 eV, we used 98 target configurations: $1s^22s^2nl$ and $1s^22s2pnl$ with $n=2-11, l=0-4$ and $1s^22p^2nl$ with $n=2-5, l=0-3$. These configurations produce 476 LS terms, all of which were used in our close-coupling expansion. The present calculations were performed using parallel R-matrix codes [19,20] developed from extensively modified versions of the RMATRIX I suite of programs [21]. We included partial waves from $L=0-11$ which resulted in a maximum of 1342 channels and Hamiltonian matrices in excess of $60\,000 \times 60\,000$. The contributions from higher partial waves ($L \geqslant 12$) were estimated for dipole transitions using the method developed by Burgess [22] and for nondipole transitions using a geometric series in L. The total ionization cross section was determined from the sum of all excitation cross sections to terms above the ionization limit.

Integral cross sections for the electron-impact total ionization of the $B(1s^22s^22p)$ ground configuration are presented in Fig. 4. The current 476 LS-term RMPS results are found to lie substantially below the previous 60 LS-term RMPS results [10]. The vastly increased number of pseudostates in the current RMPS calculation has provided a more accurate representation of continuum coupling effects. We note that the "features" in both RMPS calculations are a mixture of thresholds associated with excitation to true autoionizing states and continuum pseudostates. As the size of the calculations are further increased the true autoionizing state features will persist, while the continuum pseudostate features will smooth out.

In the RMPS calculations, LS terms involving both spectroscopic orbitals and pseudo-orbitals lie above the ionization threshold and are strongly mixed through configuration-interaction. Thus, there is no reliable method known to separate the direct ionization and excitation-autoionization contributions to the total ionization cross section. In the TDCC calculations, accurate predictions can be made for the $2p$ and $2s$ subshell direct ionization cross sections, but one cannot extract an accurate prediction for the excitation-autoionization contributions since the $1s^22s2p^2$ excited configuration straddles the $2p$ ionization threshold. However, by comparing the RMPS total ionization cross section with the TDCC direct ionization cross section, we can infer an accurate magnitude for the total excitation-autoionization contributions. The RMPS/TDCC total excitation-autoionization contribution is found to lie slightly below the plane-wave Born calculation [7] for the $1s^22s^22p\ ^2P^o \rightarrow 1s^22s2p^2\ ^2P^e$ transition, as shown in Fig. 3. However, we estimate that the $1s^22s^22p\ ^2P^o \rightarrow 1s^22s2p^2\ ^2P^e$ excitation-autoionization contribution makes up only about half of the RMPS/TDCC total $2s \rightarrow nl$ ($n \geqslant 2$) excitation-autoionization contributions.

In summary, large-scale nonperturbative TDCC and

RMPS calculations were carried out for the electron-impact ionization of the $1s^2 2s^2 2p$ ground configuration of the neutral B atom. The TDCC calculations for direct ionization of the $2s$ and $2p$ subshells of B were found to rule out electrostatic potential shape resonances found using a certain type of distorted-wave method. The current 476 LS-term RMPS calculation for the total ionization of B was found to be substantially smaller than the previous 60 LS term RMPS calculation [10] due to a more accurate treatment of continuum coupling effects. RMPS/TDCC combined calculations for the total excitation-autoionization contributions in B were found to be substantially smaller than distorted-wave calculations due to strong coupling among the configuration-interaction mixed excited states. We note that the RMPS total cross section is in reasonable agreement with the total cross section recommended by Kim and Stone [7], which was obtained from semiempirical binary encounter calculations that underestimated the $2p$ subshell direct ionization and overestimated the $2s$ subshell direct ionization, while only including a plane-wave Born calculation for the $1s^2 2s^2 2p\ ^2P^o \rightarrow 1s^2 2s 2p^2\ ^2P^e$ excitation-autoionization contribution. Our prediction of the electron-impact ionization of the B atom, combined with further excitation and ionization calculations along the B isonuclear sequence, will provide an accurate atomic database for collisional-radiative calculations of line emission in B plasmas. Diagnostics of plasma performance on existing tokamaks will then help decide whether "boronization" of heavy metal facing components could be used effectively for ITER. We hope this theoretical study will also stimulate atomic measurements of the interesting direct and indirect cross section features found in the electron-impact ionization of the neutral B atom.

This work was supported in part by grants from the U.S. Department of Energy. Computational work was carried out at the National Energy Research Scientific Computing Center in Oakland, California and at the National Center for Computational Sciences in Oak Ridge, Tennessee.

[1] *Nuclear Fusion Research: Understanding Plasma–Surface Interactions*, edited by R. E. H. Clark and D. H. Reiter (Springer, Berlin, 2005).
[2] B. Lipschultz, Y. Lin, M. L. Reinke, A. Hubbard, I. H. Hutchinson, J. Irby, B. LaBombard, E. S. Marmar, K. Marr, J. L. Terry, S. M. Wolfe, the Alcator C-Mod group, and D. Whyte, Phys. Plasmas **13**, 056117 (2006).
[3] J. Huang, B. N. Wan, J. G. Li, X. Z. Gong, X. D. Zhang, Z. W. Wu, Q. Zhou, and the HT-7 team, Nucl. Fusion **46**, 262 (2006).
[4] J. Colgan, M. S. Pindzola, D. M. Mitnik, D. C. Griffin, and I. Bray, Phys. Rev. Lett. **87**, 213201 (2001).
[5] D. V. Fursa and I. Bray, J. Phys. B **30**, L273 (1997).
[6] J. Colgan, S. D. Loch, M. S. Pindzola, C. P. Ballance, and D. C. Griffin, Phys. Rev. A **68**, 032712 (2003).
[7] Y. K. Kim and P. M. Stone, Phys. Rev. A **64**, 052707 (2001).
[8] R. E. H. Clark and J. Abdallah, Phys. Scr. **62**, 7 (1996).
[9] C. P. Ballance, D. C. Griffin, K. A. Berrington, and N. R. Badnell, J. Phys. B **40**, 1131 (2007).
[10] P. J. Marchalant and K. Bartschat, J. Phys. B **30**, 4373 (1997).
[11] M. S. Pindzola *et al.*, J. Phys. B **40**, R39 (2007).
[12] S. M. Younger, Phys. Rev. A **22**, 111 (1980).
[13] H. Jakubowicz and D. L. Moores, J. Phys. B **14**, 3733 (1981).
[14] S. M. Younger, Phys. Rev. A **35**, 2841 (1987).
[15] J. Botero and J. H. Macek, J. Phys. B **24**, L405 (1991).
[16] M. S. Pindzola, D. C. Griffin, and J. H. Macek, Phys. Rev. A **51**, 2186 (1995).
[17] D. L. Moores, Phys. Scr., T **62**, 19 (1996).
[18] N. R. Badnell, J. Phys. B **30**, 1 (1997).
[19] D. M. Mitnik, M. S. Pindzola, D. C. Griffin, and N. R. Badnell, J. Phys. B **32**, L479 (1999).
[20] C. P. Ballance and D. C. Griffin, J. Phys. B **37**, 2943 (2004).
[21] K. A. Berrington, W. B. Eissner, and P. H. Norrington, Comput. Phys. Commun. **92**, 290 (1995).
[22] A. Burgess, J. Phys. B **7**, L364 (1970).